Annales
Geophysicae
Open Access

The far-ultraviolet main auroral emission at Jupiter – Part 1: Dawn–dusk brightness asymmetries

B. Bonfond[1,*], J. Gustin[1], J.-C. Gérard[1], D. Grodent[1], A. Radioti[1], B. Palmaerts[1,2], S. V. Badman[3], K. K. Khurana[4], and C. Tao[5]

[1]Laboratoire de Physique Atmosphérique et Planétaire, Université de Liège, Allée du 6 Août, 19c, 4000 Liège, Belgium
[2]Max-Planck-Institut für Sonnensystemforschung, Justus-von-Liebig-Weg 3, 37077 Göttingen, Germany
[3]Lancaster University, Department of Physics, Lancaster, UK
[4]University of California, Los Angeles, Los Angeles, California, USA
[5]Institut de Recherche en Astrophysique et Planétologie, Toulouse, France
[*] Invited contribution by B. Bonfond, recipient of the EGU Division Outstanding Young Scientists Award 2015.

Correspondence to: B. Bonfond (b.bonfond@ulg.ac.be)

Abstract. The main auroral emission at Jupiter generally appears as a quasi-closed curtain centered around the magnetic pole. This auroral feature, which accounts for approximately half of the total power emitted by the aurorae in the ultraviolet range, is related to corotation enforcement currents in the middle magnetosphere. Early models for these currents assumed axisymmetry, but significant local time variability is obvious on any image of the Jovian aurorae. Here we use far-UV images from the Hubble Space Telescope to further characterize these variations on a statistical basis. We show that the dusk side sector is ~ 3 times brighter than the dawn side in the southern hemisphere and ~ 1.1 brighter in the northern hemisphere, where the magnetic anomaly complicates the interpretation of the measurements. We suggest that such an asymmetry between the dawn and the dusk sectors could be the result of a partial ring current in the nightside magnetosphere.

Keywords. Atmospheric composition and structure (airglow and aurora) – magnetospheric physics (auroral phenomena; current systems)

1 Introduction

The aurorae at Jupiter consist of several distinct features of various sizes, shapes, and locations (see reviews by Grodent, 2015; Delamere et al., 2014, and references therein). Studies dedicated to specific features confirmed that their gener-

ation mechanisms are indeed different and, to a large extent, independent. One of the most persistent and easily identifiable feature of Jupiter's aurorae consists of a bright and essentially closed auroral curtain around each magnetic pole, sometimes called the main oval. However, this shape can also be strongly disturbed, showing patchy patterns, as well as forks or parallel arcs (Grodent et al., 2003; Nichols et al., 2009), which is why, following Grodent et al. (2008a), we will refer to it as the main emission here below. It should also be noted that this main emission, despite its name, generally accounts for approximately half of the total emitted auroral power in the far UV (FUV). Moreover, the section of the main emission ranging between 08:00 and 13:00 magnetic local time, dubbed the discontinuity, is typically 90 % dimmer than the maximum of the main emission (Radioti et al., 2008a). While most of the main emission is generally stable over timescales of several tens of minutes, the discontinuity region exhibits transient small-scale (of a few degrees) structures (Palmaerts et al., 2015), probably associated with regions of localized velocity shear in the middle dayside magnetosphere. In the southern hemisphere, the auroral statistical contour is roughly oval-shaped. In the north, a magnetic anomaly around 100° System III (S$_{\mathrm{III}}$) longitude distorts the contour into a kidney bean shape (Grodent et al., 2008a).

While at Earth and at Saturn the inner boundary of the main auroral oval magnetically maps just inward of the magnetopause, the main emission at Jupiter magnetically maps to the middle magnetosphere at L shells between 20 and 60 Jo-

vian radii (R_J) (Vogt et al., 2011). The main auroral emission at Jupiter is the signature of the corotation enforcement currents coupling the magnetosphere to the ionosphere (Cowley and Bunce, 2001; Hill, 2001; Southwood and Kivelson, 2001). Most of the plasma in the Jovian magnetosphere originates from the volcanic moon Io. Initially neutral gas particles are dissociated and/or ionized before they end up frozen in the rapidly rotating magnetic field of the planet (e.g., Dols et al., 2008). As this plasma migrates outward because of instabilities driven by centrifugal force and pressure gradients, it progressively sub-corotates and bends the magnetic field azimuthally backward. The resulting electric current forms a loop made of latitudinal equatorward (Pedersen) currents in the planetary ionosphere, radial outward currents in the magnetospheric plasma sheet and field-aligned currents in between to close the circuit. In the plasma sheet, the Lorentz force resulting from the radial currents accelerates the plasma azimuthally towards corotation. The upward field-aligned corotation enforcement currents reach a maximum close to the L shell, beyond which the plasma begins to significantly sub-corotate. The resulting quasi-static electric field accelerates electrons downward into the atmosphere, which ultimately generates the main auroral emission. Ray et al. (2014) provide an excellent review of the successive evolutions of the analytical models describing these currents, and Chané et al. (2013) do the same for the magneto-hydrodynamic (MHD) numerical simulations. The size of the main emission contour changes from one day to another, but it also experiences significant variations on a timescale of months (Grodent et al., 2008b; Bonfond et al., 2012). Comparisons with the location of the Ganymede auroral footprint relative to the main emission showed that these size variations are due to a combination of a varying field line stretching due to the plasma sheet changes through time and because the corresponding L shell also changes with time. Such long-term trends have been attributed to variations in the outgasing rate at Io, which could modify both the mass outflow rate and the plasma sheet density (Bonfond et al., 2012).

Even though its generation mechanism is independent from the solar wind, the main emission still responds to solar wind variations such as the arrival of a shock compressing the magnetosphere or subsequent expansion of the magnetosphere (Nichols et al., 2007). This response appears in the form of a brightening of both polar and main emissions, combined with a strong distortion of the dusk part of the main emission. However, not all brightenings of the main emission are triggered by solar wind variations. Brightness enhancements of the dawn portion of the main emission, called dawn storms, can increase to 1.8 MR, i.e., approximately 4 times the brightness observed in normal conditions, and last for a couple of hours (e.g., Gustin et al., 2006). During the large Hubble Space Telescope campaign dedicated to Jupiter's aurorae concurrent with the New Horizons flyby, dawn storms were seen both during periods of both compressed and rarefied solar wind conditions (Nichols et al., 2009).

Another way the solar wind interferes with the corotation enforcement process is through the basic shape of the magnetosphere and the subsequent local time variations in magnetic field topology and the plasma flow around the planet. Two different strategies have been used so far to account for such local time variations: 3-D MHD simulations of the magnetosphere (Walker and Ogino, 2003; Chané et al., 2013) or 1-D models of the magnetosphere–ionosphere coupling adapted for every hour in local time (Ray et al., 2014). The analytical model of the auroral currents by Ray et al. (2014) predicts that they shall be strongest in the dawn sector with values at least 1 order of magnitude larger than in the noon-to-dusk sector. These authors however note that their 1-D model only accounts for the variations in the normal component of the magnetic field in the equatorial plane but does not account for the azimuthal bendback of the magnetic field lines nor the presence of azimuthal currents. On the other hand, the MHD simulations (e.g., Walker and Ogino, 2003; Chané et al., 2013) do not show such a crisp difference and instead predict stronger field-aligned currents on the dusk side, and hence brighter related aurorae, than in the dawn sector. In order to resolve the discrepancy between these two approaches, we make use of the set of Hubble Space Telescope far-UV images to perform a statistical comparison of the main emission brightness in the dawn and dusk sectors and we draw conclusions on the underlying current system. The altitude of the main emission and its possible variations with local time are discussed in the second part of this paper (Bonfond et al., 2015).

2 Dawn–dusk variations in the main emission brightness

The present study relies on a set of 1663 images acquired with the Hubble Space Telescope's (HST) Advanced Camera for Surveys (ACS). 1036 were acquired in the northern hemisphere and 627 in the southern hemisphere. The definition of the sub-domains of the ultraviolet range depends on the field of study. In the context of the studies of the Jovian aurorae, the FUV range covers wavelengths from the Lyman-α line (121.6 nm) to 170 nm. Hence, it also includes the Werner and Lyman bands of the H_2 molecule. Approximately 10 % of the precipitated energy is converted into H_2 ultraviolet emissions. Around half of these ultraviolet emissions is emitted in the extreme-UV (EUV) range and the other half is emitted in the FUV range. Moreover, Lyman-α line emission from atomic hydrogen, most of which originates from the dissociative excitation of H_2, is also present in this spectral domain and typically reaches 10 % of the total (i.e., extreme + far UV) H_2 ultraviolet emissions (Gustin et al., 2012).

For the present study, ACS images are preferred to images from the Space Telescope Imaging Spectrograph (STIS) because ACS images are more affected by the "red leak", i.e., the "lower than expected" light rejection at a higher
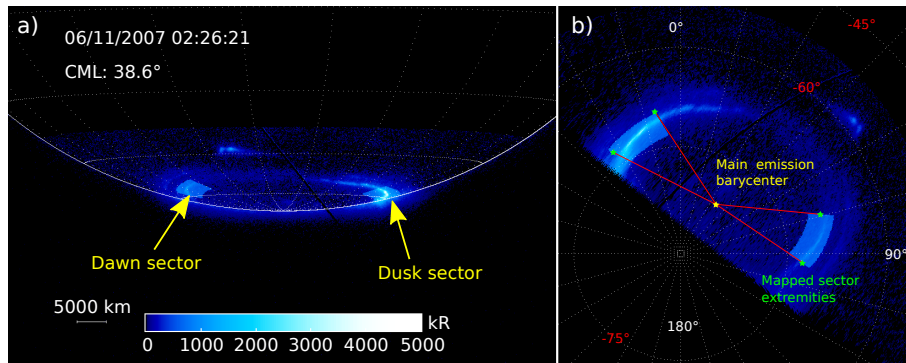
Figure 1. Panel **(a)** shows a background subtracted HST ACS image of the southern aurora of Jupiter. The brightness of the two sectors of interest has been enhanced. The emitted power is extracted from this image. As shown on panel **(b)**, the two sectors of interest are latitudinally defined according to the appropriate reference contour for the main emission, and their longitudinal extent corresponds to sectors 2 local-time hour long on the dawn and dusk side projected into the ionosphere along magnetic field lines following the model of Vogt et al. (2015) with VIPAL for a radial distance of 30 R$_J$. These mapped positions are shown with green stars.

(near-UV and visible) wavelength (Boffi et al., 2008). These higher-wavelength photons impacting the detectors originate from the Rayleigh scattering of the solar light by Jupiter's neutral atmosphere. This background planetary disk results in both a lower signal-to-noise ratio for the auroral emissions in which we are interested and in a crisper planetary limb corresponding to the visible limb located at the 1 bar level. As a consequence, the location of the planetary center is determined assuming that the limb on the image corresponds to the 1 bar level ellipsoid with an equatorial radius of 71 492 km and a polar radius of 66 854 km.

It should be noted that this data set is not evenly sampled in terms of central meridian longitude (CML). Because of the tilt of the Jovian magnetic field, some sub-Earth longitude ranges provide a better visibility of the aurorae than others, depending on the hemisphere. Hence, CMLs between 110 and 230° S$_{III}$ have been preferentially observed in the north, while CMLs between 300 and 120° S$_{III}$ have been preferred for the south. Additionally, the favored orientation for the northern aurorae's observations is such that, most of the time, the magnetic anomaly (around $\sim 100°$ S$_{III}$) is located in the dusk sector, making it challenging to disentangle local time effects from the consequences of localized variations in the magnetic field amplitude in the ionosphere for the current system.

Estimating the emitted power corresponding to an auroral feature on HST images is easier than estimating their brightness as seen from above because the power does not need to be corrected for limb brightening. The first step consists in removing the planetary disk background from the image, according to the method described in Bonfond et al. (2011). Then, measuring the emitted power only requires adding the counts in the region of interest and multiplying the total by the appropriate conversion coefficient accounting for the instrumental transmission, a typical color ratio of 2.5 and the actual Earth–Jupiter distance (Gustin et al.,

2012). Our method relies on the automatic selection of two strip-shaped regions of interest (ROIs), one for dawn and one for dusk, centered on the monthly mean reference oval corresponding to the epoch of the observation (Bonfond et al., 2012) (see Fig. 1). Our dawn and dusk sectors correspond to the local time sectors ranging from 06:00 to 08:00 and from 16:00 to 18:00 in the equatorial plane, respectively, thus avoiding the discontinuity. The latitudinal width of the ROIs does not significantly affect the measured power as long as the whole main emission curtain width falls within the strip's boundaries. The chosen width corresponds to $\sim 3°$ of latitude, which encompasses the typical day-to-day variability in the main emission location but avoids the selection of significant portions of outer or polar emissions. The longitudinal boundaries of the ROIs correspond to the mapping of boundaries of the equatorial local time sectors at a radial distance of 30 R$_J$ using the mapping model from Vogt et al. (2015) based on the VIPAL model (Hess et al., 2011). As a consequence, the two ROIs do not cover an equal area on the planet because of the asymmetry of the magnetic field on the surface of the planet. The pixels corresponding to the ROIs are then identified in the background-subtracted image and the emitted power is integrated over these two areas. Images in which at least one of the two sectors cannot be completely seen are excluded from our analysis. It should be noted that the strips are wide enough to occasionally include either the Ganymede footprint (Clarke et al., 2002) or polar dawn spots (Radioti et al., 2008b). However, the power of these features is small compared to the total emitted power in the selected sectors (< 1 GW compared to ~ 50 GW), so they do not affect our conclusions.

Figure 2 shows the dusk / dawn power ratio in the northern and the southern hemispheres. In the southern hemisphere, the dusk side is brighter than the dawn side in 496 cases out of 534 and the median ratio is 3.1. Since they are not affected by the magnetic anomaly and its related uncertain-
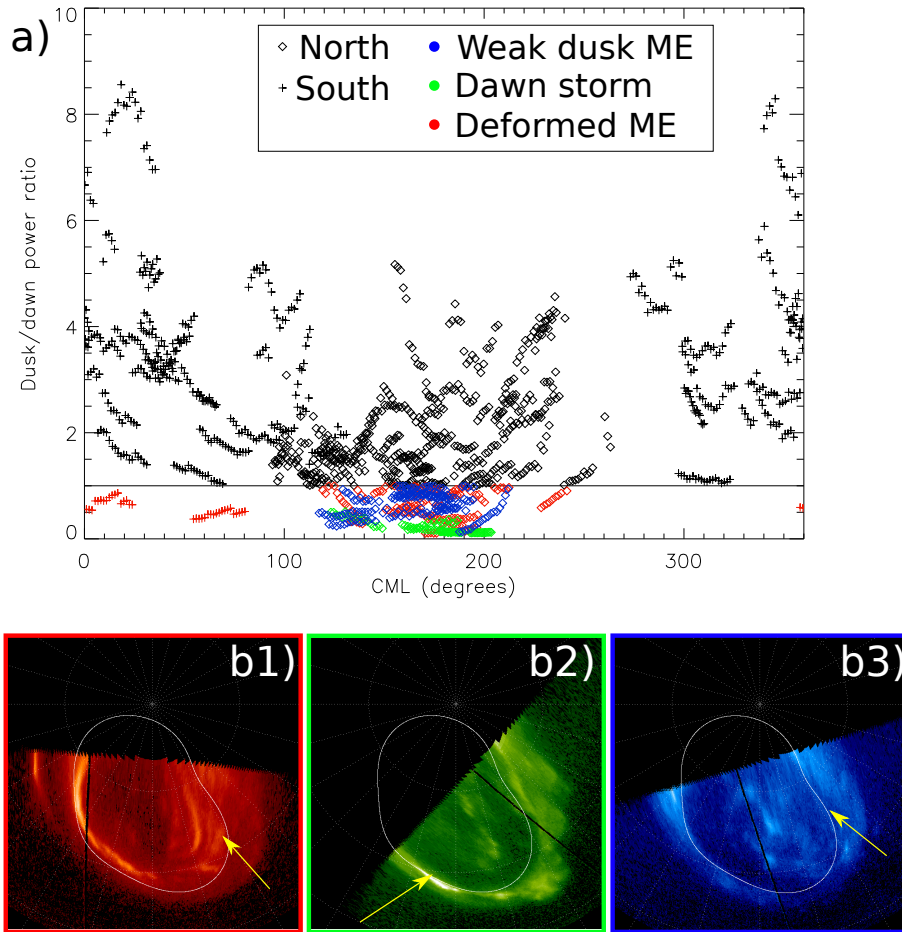
Figure 2. Panel **(a)**: plot of the ratio of the integrated emitted power in the 16:00 to 18:00 LT sector (dusk side) over the 06:00 to 08:00 LT sector (dawn side) for the northern (diamonds) and southern (pluses) hemispheres. Panels **b1–b3**: polar projection of examples of the three classes of cases for which the dusk sector is weaker than the dawn sector. The first case is a case of strongly disturbed main emission, the second one is a dawn storm and the third case simply displays an unusually weak dusk arc. The arrow on the first image highlights the dawn arc while, on the last two images, the arrows highlight the expected location of the main emission.

ties (see below), the southern values probably display a reliable picture of the field-aligned currents pattern associated with the main emission. In the northern hemisphere, the dusk side is brighter than the dawn side in 516 cases out of 956. However, the overall median ratio between the dusk and the dawn side is 1.1 and the emitted power in these two sectors is actually fairly similar. Unfortunately, as clearly demonstrated by the bottom plot of Fig. 5 in Gérard et al. (2013), the variations in the magnetic field magnitude (and orientation) along the main emission are much larger in the northern hemisphere than in the southern one. Indeed, in the CML range from ~ 120 to $220°$ S_{III}, the magnetic anomaly distorts the magnetic field lines in such a way that the extent of the dusk ROI along the reference oval is up to twice as small as the extent of the corresponding dawn ROI. Possible but currently unknown inaccuracies in the magnetic field model would thus have a significant impact in the measured dusk-to-dawn power ratio. More importantly, the impact of

the ionospheric magnetic field strength on the precipitated energy flux remains unclear (Gérard et al., 2013), which prevents clear interpretations.

Our results, and especially those regarding the southern hemisphere, indicate that the dusk side of the main emission is generally brighter than the dawn side. These results are consistent with both the results from MHD simulations and the estimates of the field-aligned currents derived from equatorial magnetic field measurements (Khurana, 2001). However, they are not consistent with the corotation enforcement currents 1-D model of Ray et al. (2014), which predicts stronger currents on the dawn side. According to Tao et al. (2010), one partial explanation could be the difference in Pedersen conductivity in the dusk sector compared to the dawn sector due to the different history of the solar EUV illumination. Another possibility, likely to have a stronger effect on the auroral currents, could be the presence of an additional partial ring current in the nightside middle magnetosphere as
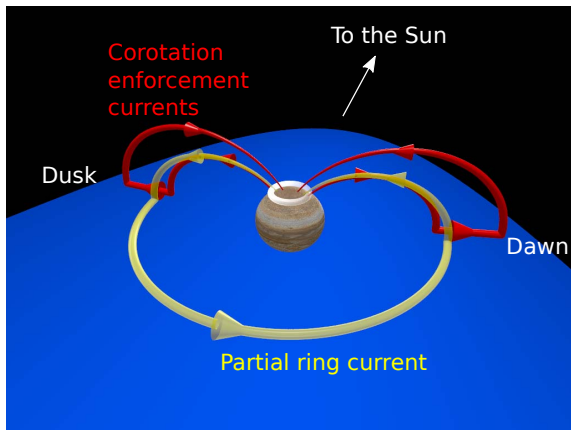
Figure 3. Scheme of the two current systems suggested to affect the main emission brightness. The blue area represents the magnetosphere and the Sun is towards the top. The corotation enforcement current loops are present at all local times, albeit with varying intensity, but only the dawn and the dusk loops are shown. In this illustration, the two currents systems are slightly shifted and only the northern current loops are shown for clarity. It can be see that on the dusk side, the currents of the lower latitude field-aligned branches flow in the same direction, thus leading to a brighter aurora, while the currents on the dawn side flow in the opposite direction, leading to a dimmer aurora. For clarity, only the northern current systems are shown.

discussed by Khurana (2001) (see Fig. 3). According to this study, the divergence of the magnetic field components indicates the presence of significant downward currents (i.e., towards the ionosphere) on the dawn side and upward currents on the dusk side. Thus the field-aligned branches of such a current system would be opposed to corotation field-aligned currents on the dawn side and reenforce the upward field-aligned currents on the dusk side, consistent with our auroral brightness observations.

Whatever the hemisphere, the cases for which the dawn emissions are brighter may be sorted into three classes. The first one corresponds to cases where the dusk part of the main emission displays a distorted pattern and appears to be pushed poleward of its usual location (155 images in the north and 38 in the south, Fig. 2b1). In these cases, it is not clear what belongs to the main emission and what belongs to the polar region. Hence it is not clear whether the dusk side of the main emission has actually dimmed or whether it has just moved inward. These peculiar main emission morphologies are associated with the response to the arrival of a solar wind compression region at Jupiter (Nichols et al., 2007, 2009). We note that the presence of secondary arcs could be compatible with an enhanced partial ring current loop in response to the compression of the magnetosphere. The second class corresponds to dawn storms (87 images in the north), i.e., transient spectacular enhancements of the dawn arc of the main emission (Gustin et al., 2006) (Fig. 2b2). Such auroral be-

haviors are observed regardless of the state of the solar wind input (Nichols et al., 2009). The third class is made up of cases of unusually weak dusk side main emission (198 cases in the north; Fig. 2b3).

3 Conclusions

While early models of the corotation enforcement current system that gives rise to the main auroral emission at Jupiter assumed symmetry around the magnetic axis, observations and further developments of these models now outline the importance of local time dependence. The present paper aims to characterize the local time variations in the main emission on a statistical basis, based on the large data set of FUV auroral observations carried out by the Hubble Space Telescope.

Our study focusses on the dawn–dusk variation in the FUV emitted power in the dawn and dusk sectors of the main emission. Our results show that the dusk side is generally ~ 3 times brighter than the dawn side, at least in the southern hemisphere. In the northern hemisphere, the ratio appears to be closer to unity, which is probably due to the combination of the limited CML coverage and the presence of a localized magnetic anomaly. Comparisons of quasi-simultaneous images of the Jovian aurorae in both hemispheres have already highlighted some significant brightness differences between conjugate sectors of the main emission. Unfortunately, the search for a possible (anti-)correlation with the ionospheric field magnitude was inconclusive, due to conflicting results derived from a very limited sample of image pairs (Gérard et al., 2013). Nevertheless, if the ionospheric magnetic field magnitude affects the main emission brightness, then one should also expect dependence on both local time and CML. Furthermore, the fact that the northern dusk sector, which is usually located in a region with a strong magnetic field on the ACS images, appears weaker than the southern one suggests that the emitted power is inversely proportional to the magnetic field strength. If we consider the probably more representative southern hemisphere alone, the brighter dusk side is consistent with the electric currents derived from the Galileo magnetic field measurements (Khurana, 2001) but contradicts the model results from Ray et al. (2014), which predict a brighter dawn side. Following Khurana (2001), we suggest that our results, and possibly their discrepancy with the results from the 1-D model of Ray et al. (2014), could be caused by a partial ring current on the nightside (with dawn and dusk side field-aligned current legs) that is not accounted for in their model. Because the Juno spacecraft will fly over the polar regions along a dawn–dusk orbital plane, offering a bird's eye view of the aurorae without any CML selection bias, the combination of both its remote-sensing and in situ observations should resolve the observational ambiguities discussed here, especially in the north, and thus confirm or disprove our interpretation of the dawn–dusk brightness asymmetry.

References

Boffi, F. R., Sirianni, M., Lucas, R. A., Walborn, N. R., and Proffitt, C. R.: Delivery of a new ACS SBC throughput curve for Synphot, Technical Instrument Report ACS 2008-002, STSCI, tIR ACS 2008-002, 2008.

Bonfond, B., Vogt, M. F., Gérard, J.-C., Grodent, D., Radioti, A., and Coumans, V.: Quasi-periodic polar flares at Jupiter: A signature of pulsed dayside reconnections?, Geophys. Res. Lett., 380, L02104, doi:10.1029/2010GL045981, 2011.

Bonfond, B., Grodent, D., Gérard, J.-C., Stallard, T., Clarke, J. T., Yoneda, M., Radioti, A., and Gustin, J.: Auroral evidence of Io's control over the magnetosphere of Jupiter, Geophys. Res. Lett., 39, L01105, doi:10.1029/2011GL050253, 2012.

Bonfond, B., Gustin, J., Gérard, J. C., Grodent, D., Radioti, A., Palmaerts, B., Badman, S. V., Khurana, K. K., and Tao, C.: The far-ultraviolet main auroral emission at Jupiter – Part 2: Vertical emission profile, Ann. Geophys., 33, 1211–1219, doi:10.5194/angeo-33-1211-2015, 2015.

Chané, E., Saur, J., and Poedts, S.: Modeling Jupiter's magnetosphere: Influence of the internal sources, J. Geophys. Res.-Space, 118, 2157–2172, doi:10.1002/jgra.50258, 2013.

Clarke, J. T., Ajello, J., Ballester, G., Ben Jaffel, L., Connerney, J., Gérard, J.-C., Gladstone, G. R., Grodent, D., Pryor, W., Trauger, J., and Waite, J. H.: Ultraviolet emissions from the magnetic footprints of Io, Ganymede and Europa on Jupiter, Nature, 415, 997–1000, 2002.

Cowley, S. W. H. and Bunce, E. J.: Origin of the main auroral oval in Jupiter's coupled magnetosphere-ionosphere system, Planet. Space Sci., 49, 1067–1088, doi:10.1016/S0032-0633(00)00167-7, 2001.

Delamere, P. A., Bagenal, F., Paranicas, C., Masters, A., Radioti, A., Bonfond, B., Ray, L., Jia, X., Nichols, J., and Arridge, C.: Solar Wind and Internally Driven Dynamics: Influences on Magnetodiscs and Auroral Responses, Space Sci. Rev., 187, 51–97, doi:10.1007/s11214-014-0075-1, 2014.

Dols, V., Delamere, P. A., and Bagenal, F.: A multispecies chemistry model of Io's local interaction with the Plasma Torus, J. Geophys. Res., 113, A09208, doi:10.1029/2007JA012805, 2008.

Gérard, J.-C., Grodent, D., Radioti, A., Bonfond, B., and Clarke, J. T.: Hubble observations of Jupiter's north-south conjugate ultraviolet aurora, Icarus, 226, 1559–1567, doi:10.1016/j.icarus.2013.08.017, 2013.

Grodent, D.: A Brief Review of Ultraviolet Auroral Emissions on Giant Planets, Space Sci. Rev., 187, 23–50, doi:10.1007/s11214-014-0052-8, 2015.

Grodent, D., Clarke, J. T., Kim, J., Waite, J. H., and Cowley, S. W. H.: Jupiter's main auroral oval observed with HST-STIS, J. Geophys. Res., 108, 2–1, doi:10.1029/2003JA009921, 2003.

Grodent, D., Bonfond, B., Gérard, J.-C., Radioti, A., Gustin, J., Clarke, J. T., Nichols, J., and Connerney, J. E. P.: Auroral evidence of a localized magnetic anomaly in Jupiter's northern hemisphere, J. Geophys. Res., 113, A09201, doi:10.1029/2008JA013185, 2008a.

Grodent, D., Gérard, J.-C., Radioti, A., Bonfond, B., and Saglam, A.: Jupiter's changing auroral location, J. Geophys. Res., 113, A01206, doi:10.1029/2007JA012601, 2008b.

Gustin, J., Cowley, S. W. H., Gérard, J.-C., Gladstone, G. R., Grodent, D., and Clarke, J. T.: Characteristics of Jovian morning bright FUV aurora from Hubble Space Telescope/Space Telescope Imaging Spectrograph imaging and spectral observations, J. Geophys. Res.-Space, 111, A09220, doi:10.1029/2006JA011730, 2006.

Gustin, J., Bonfond, B., Grodent, D., and Gérard, J. C.: Conversion from HST ACS and STIS auroral counts into brightness, precipitated power and radiated power for H_2 giant planets, J. Geophys. Res., 117, A07316, doi:10.1029/2012JA017607, 2012.

Hess, S., Delamere, P. A., Dols, V., and Ray, L. C.: Comparative study of the power transferred from satellite-magnetosphere interactions to auroral emissions, J. Geophys. Res., 116, A01202, doi:10.1029/2010JA015807, 2011.

Hill, T. W.: The Jovian auroral oval, J. Geophys. Res., 106, 8101–8108, doi:10.1029/2000JA000302, 2001.

Khurana, K. K.: Influence of solar wind on Jupiter's magnetosphere deduced from currents in the equatorial plane, J. Geophys. Res., 106, 25999–26016, doi:10.1029/2000JA000352, 2001.

Nichols, J. D., Bunce, E. J., Clarke, J. T., Cowley, S. W. H., Gérard, J.-C., Grodent, D., and Pryor, W. R.: Response of Jupiter's UV auroras to interplanetary conditions as observed by the Hubble Space Telescope during the Cassini flyby campaign, J. Geophys. Res.-Space, 112, A02203, doi:10.1029/2006JA012005, 2007.

Nichols, J. D., Clarke, J. T., Gérard, J. C., Grodent, D., and Hansen, K. C.: Variation of different components of Jupiter's auroral emission, J. Geophys. Res.-Space, 114, A06210, doi:10.1029/2009JA014051, 2009.

Palmaerts, B., Radioti, A., Grodent, D., Chané, E., and Bonfond, B.: Transient small-scale structure in the main auroral emission at Jupiter, J. Geophys. Res. Space Physics, 119, 9931–9938, doi:10.1002/2014JA020688, 2015.

Radioti, A., Gérard, J.-C., Grodent, D., Bonfond, B., Krupp, N., and Woch, J.: Discontinuity in Jupiter's main auroral oval, J. Geophys. Res., 113, A01215, doi:10.1029/2007JA012610, 2008a.

Radioti, A., Grodent, D., Gérard, J.-C., Bonfond, B., and Clarke, J. T.: Auroral polar dawn spots: Signatures of internally driven reconnection processes at Jupiter's magnetotail, Geophys. Res. Lett., 35, L03104, doi:10.1029/2007GL032460, 2008b.

Ray, L. C., Achilleos, N. A., Vogt, M. F., and Yates, J. N.: Local time variations in Jupiter's magnetosphere-ionosphere coupling system, J. Geophys. Res.-Space, 119, 4740–4751, doi:10.1002/2014JA019941, 2014.

Southwood, D. J. and Kivelson, M. G.: A new perspective concerning the influence of the solar wind on the Jovian magnetosphere, J. Geophys. Res., 106, 6123–6130, doi:10.1029/2000JA000236, 2001.

Tao, C., Fujiwara, H., and Kasaba, Y.: Jovian magnetosphere-ionosphere current system characterized by diurnal variation of ionospheric conductance, Planet. Space Sci., 58, 351–364, doi:10.1016/j.pss.2009.10.005, 2010.

Vogt, M. F., Kivelson, M. G., Khurana, K. K., Walker, R. J., Bonfond, B., Grodent, D., and Radioti, A.: Improved mapping of Jupiter's auroral features to magnetospheric sources, J. Geophys. Res.-Space, 116, A03220, doi:10.1029/2010JA016148, 2011.

Vogt, M. F., Bunce, E. J., Kivelson, M. G., Khurana, K. K., Walker, R. J., Radioti, A., Bonfond, B., and Grodent, D.: Magnetosphere-ionosphere mapping at Jupiter: Quantifying the effects of using different internal field models, J. Geophys. Res.-Space, 120, 2584–2599 , doi:10.1002/2014JA020729, 2015.

Walker, R. J. and Ogino, T.: A simulation study of currents in the Jovian magnetosphere, Planet. Space Sci., 51, 295–307, doi:10.1016/S0032-0633(03)00018-7, 2003.